Supplementary Information

Study of temperature dependent three components dynamic covalent assembly via Hantzsch reaction catalyzed by dioxido- and oxidoperoxidomolybdenum(VI) complexes under solvent free condition

M.R. Maurya, N. Saini and F. Avecilla

Table S1 Details of the weight loss of methanol and the formation of MoO_3 in complexes and their corresponding decomposition temperature range

Compound	% MeOH			% MoO_3		
	Temp. range [°C]	Calc.	Obs.	Temp. [°C]	Calc.	Obs.
[$Mo^{VI}O_2$(ap-bhz)(MeOH)] **1**	110-220	6.5	6.4	550	29.1	28.9
[$Mo^{VI}O_2$(ap-inh)(MeOH)] **2**	147-210	6.5	6.3	510	29.1	28.6
[$Mo^{VI}O_2$(ap-nah)(MeOH)] **3**	125-200	6.5	6.4	530	29.1	28.7
[$Mo^{VI}O_2$(ap-fah)(MeOH)] **4**	141-215	6.6	6.6	540	29.8	28.6
[$Mo^{VI}O(O_2)$(ap-bhz)(MeOH)] **5**	132-225	6.3	6.4	528	28.2	27.6
[$Mo^{VI}O(O_2)$(ap-inh)(MeOH)] **6**	149-220	9.4	9.5	516	28.2	27.9
[$Mo^{VI}O(O_2)$(ap-nah)(MeOH)] **7**	122-190	6.3	6.7	531	28.2	27.3
[$Mo^{VI}O(O_2)$(ap-fah)(MeOH)] **8**	129-215	9.6	9.8	537	28.8	28.1

Table S2 Crystal Data and Structure Refinement for the complex [$Mo^{VI}O_2$(ap-bhz)(DMSO)] **1a**

	1a (CCDC 1436144)
Formula	C_{21} H_{22} Mo N_4 O_5 S
Formula weight	538.43
T, *K*	296(2)
Wavelength, Å	0.71073
Crystal system	Monoclinic
Space group	C2/c
a/Å	26.895(4)
b/Å	8.4616(10)
c/Å	21.724(3)
β/°	110.874(8)
V/Å^3	4619.3(10)
Z	8

F_{000}	2192
D_{calc}/g cm^{-3}	1.548
μ/mm^{-1}	0.698
θ/ (º)	1.62 to 28.31
R_{int}	0.0996
Crystal size/ mm^3	0.21× 0.17 × 0.14
Goodness-of-fit on F^2	0.971
$R_1[I>2\sigma(I)]$ [a]	0.0571
wR_2 (all data) [b]	0.1694
Largest differences peak and hole (eÅ^{-3})	0.408 and -0.422

[a] $R_1 = \Sigma ||F_o| - |F_c|| / \Sigma |F_o|$. [b] $wR_2 = \{\Sigma[w(|F_o|^2 - |F_c|^2)^2] / \Sigma[w(F_o^2)^2]\}^{1/2}$

Table S3 Bond lengths and angles for the compound [$Mo^{VI}O_2$(ap-bhz)(DMSO)] **1a**

Bond lengths	**1a**
Mo(1)-O(1)	1.690(4)
Mo(1)-O(2)	1.684(4)
Mo(1)-O(3)	1.970(4)
Mo(1)-O(4)	1.963(4)
Mo(1)-N(3)	2.273(5)
Mo(1)-O(5)	2.304(4)
N(1)-C(1)	1.337(7)
N(1)-N(2)	1.417(7)
N(1)-C(14)	1.429(7)
N(2)-C(3)	1.341(7)

Angles	**1a**
O(1)-Mo(1)-O(2)	105.3(2)
O(1)-Mo(1)-O(3)	95.21(19)
O(2)-Mo(1)-O(3)	98.67(19)
O(1)-Mo(1)-O(4)	102.87(18)
O(2)-Mo(1)-O(4)	97.09(19)
O(3)-Mo(1)-O(4)	151.90(19)
O(1)-Mo(1)-N(3)	159.51(18)
O(2)-Mo(1)-N(3)	92.46(18)
O(3)-Mo(1)-N(3)	71.66(19)
O(4)-Mo(1)-N(3)	84.58(18)
O(1)-Mo(1)-O(5)	87.63(17)
O(2)-Mo(1)-O(5)	167.04(17)
O(3)-Mo(1)-O(5)	80.61(16)
O(4)-Mo(1)-O(5)	78.86(16)
N(3)-Mo(1)-O(5)	74.97(14)

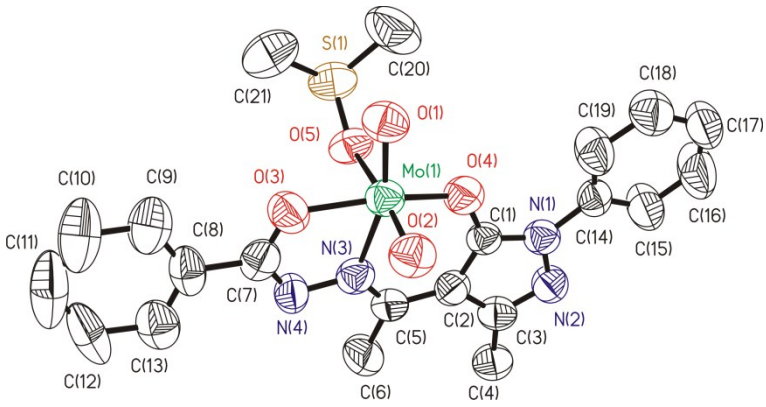

Fig. S1 ORTEP plot of complex [$Mo^{VI}O_2$(ap-bhz)(DMSO)] **1a**. All the non-hydrogen atoms are presented by their 50% probability ellipsoids. Hydrogen atoms are omitted for clarity.

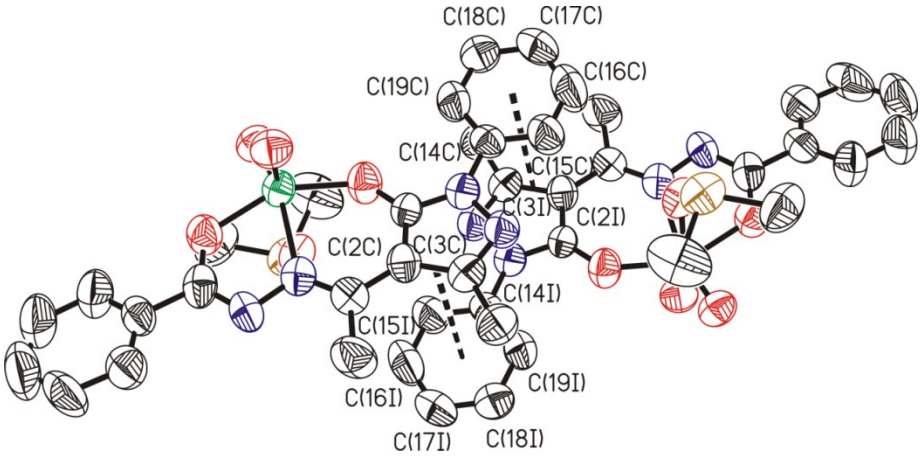

Fig. S2 Intermolecular π-π interactions in **1a**. Dashed lines link the centres of the π clouds involving in each interaction.

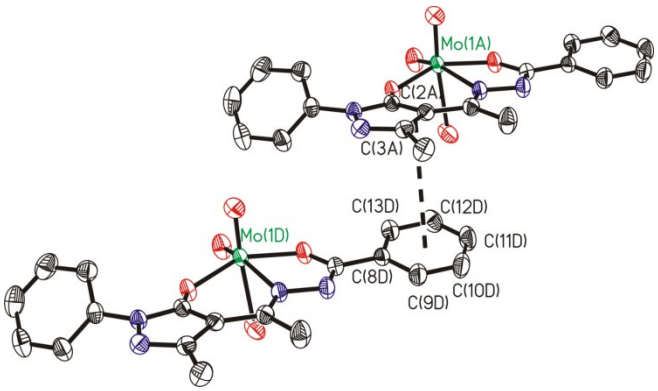

Fig. S3 Intermolecular π-π interactions in **1b**. Dashed lines link the centres of the π clouds involving in each interaction.

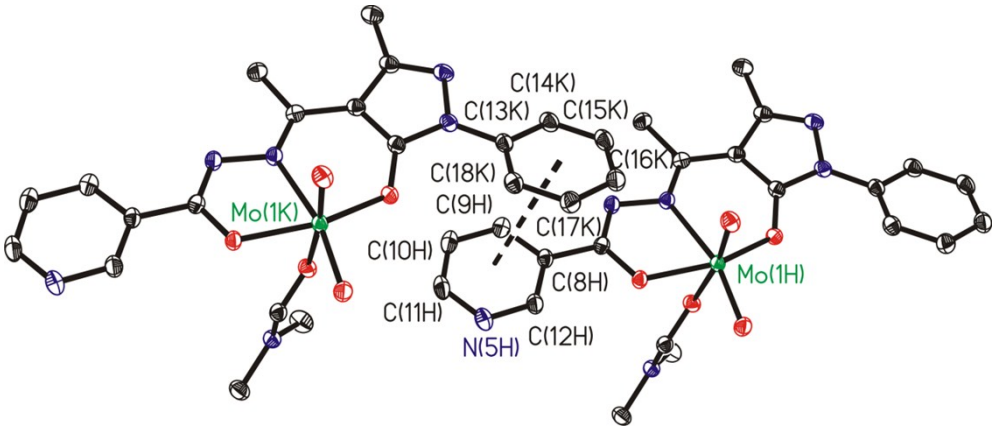

Fig. S4 Intermolecular π-π interactions in **3a**. Dashed lines link the centres of the π clouds involving in each interaction.

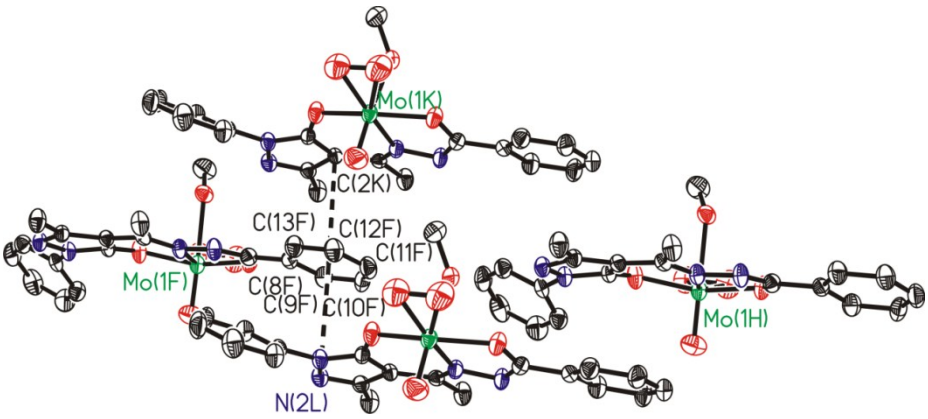

Fig. S5 Intermolecular π-π interactions in **5**. Dashed lines link the centres of the π clouds involving in each interaction.

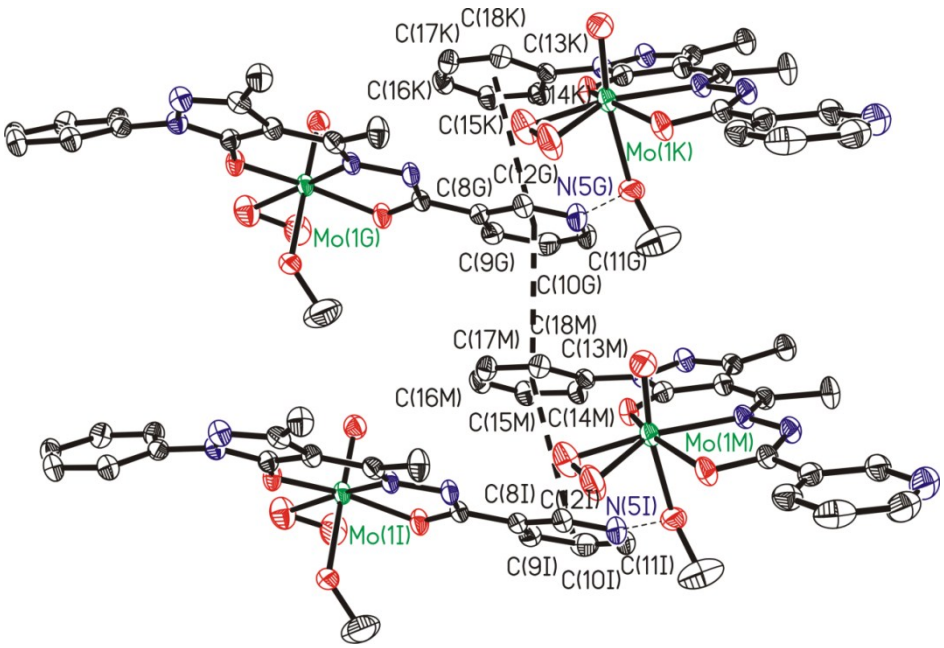

Fig. S6 Intermolecular π-π interactions in **7a**. Dashed lines link the centres of the π clouds involving in each interaction.

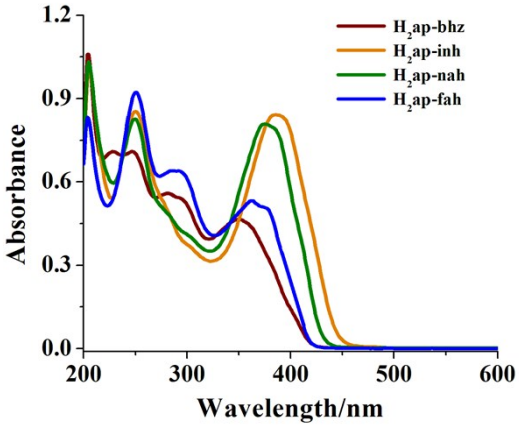

Fig. S7 UV-vis spectra of H_2ap-bhz **I** (conc. 3.9×10^{-4} M), H_2ap-inh **II** (conc. 3.4×10^{-4} M), H_2ap-nah **III** (conc. 3.0×10^{-4} M) and H_2ap-fah **IV** (conc. 3.6×10^{-4} M) recorded in methanol solution.

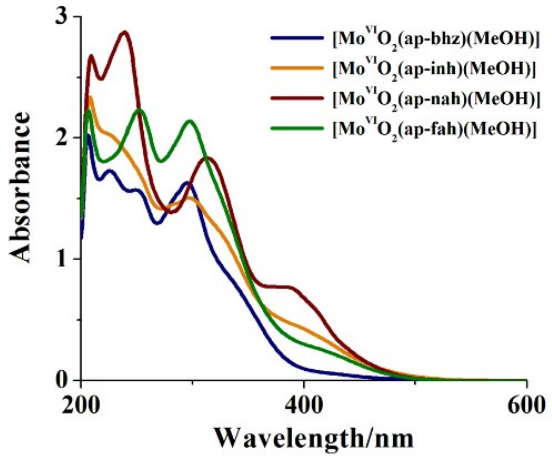

Fig. S8 UV-vis spectra of four dioxidomolybdenum(VI) complexes, **1**(conc. 2.0×10^{-4} M), **2** (conc. 2.5×10^{-4} M), **3** (conc. 3.3×10^{-4} M) and **4** (conc. 2.7×10^{-4} M) recorded in methanol.

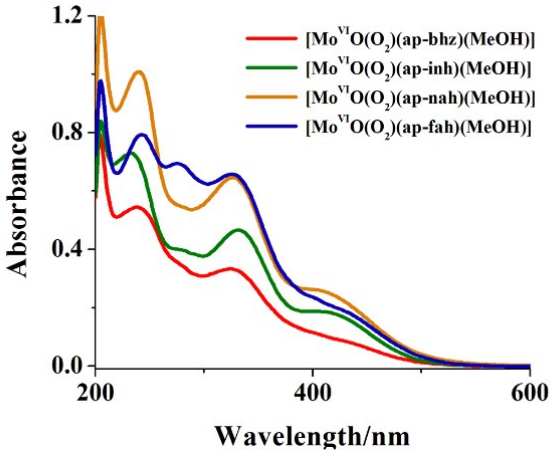

Fig. S9 UV-vis spectra of four oxidoperoxidomolybdenum(VI) complexes, **5** (conc. 3.1×10^{-4} M), **6** (conc. (2.2×10^{-4} M), **7** (conc. 2.3×10^{-4} M) and **8** (conc 3.5×10^{-4}M) recorded in methanol.

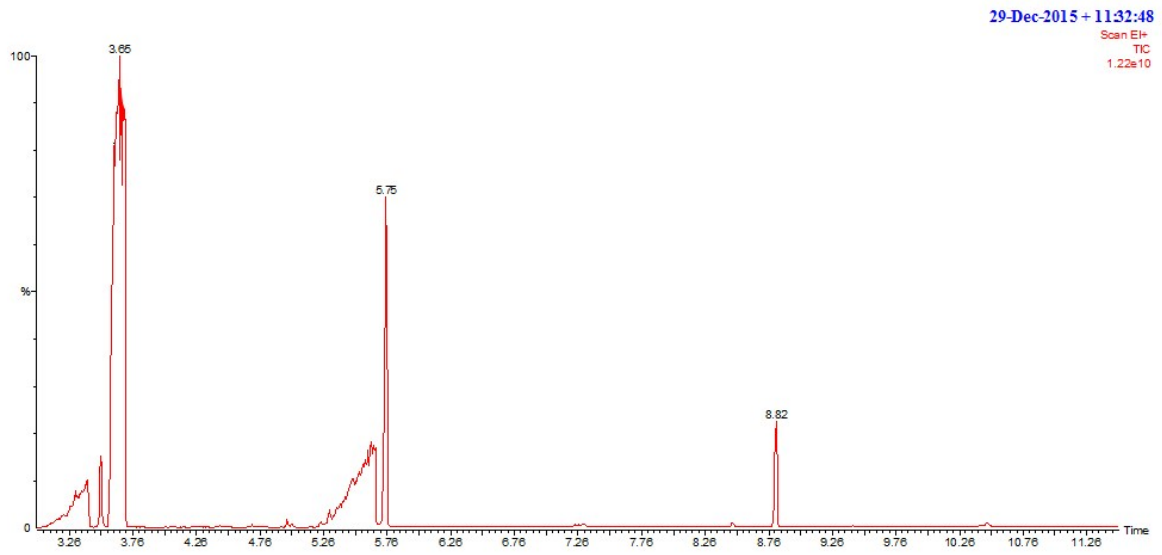

Fig. S10 (a) GC-MS chromatogram of Step-1 (Hantzsch reaction mechanism) depicting three prominent peaks at retention time 3.65, 5.75 and 8.82 min, corresponding to methylacetoacetate, benzaldehyde and methyl-2-benzylidene-3-oxobutanoate respectively.

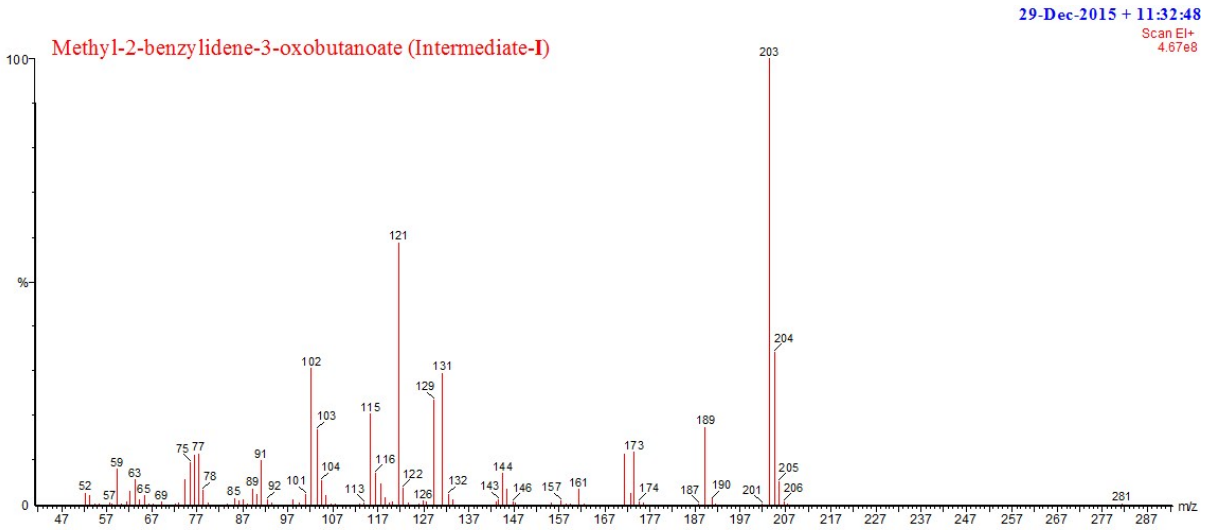

Fig. S10 (b) GC-MS chromatogram of methyl-2-benzylidene-3-oxobutanoate (Intermediate-**I**)

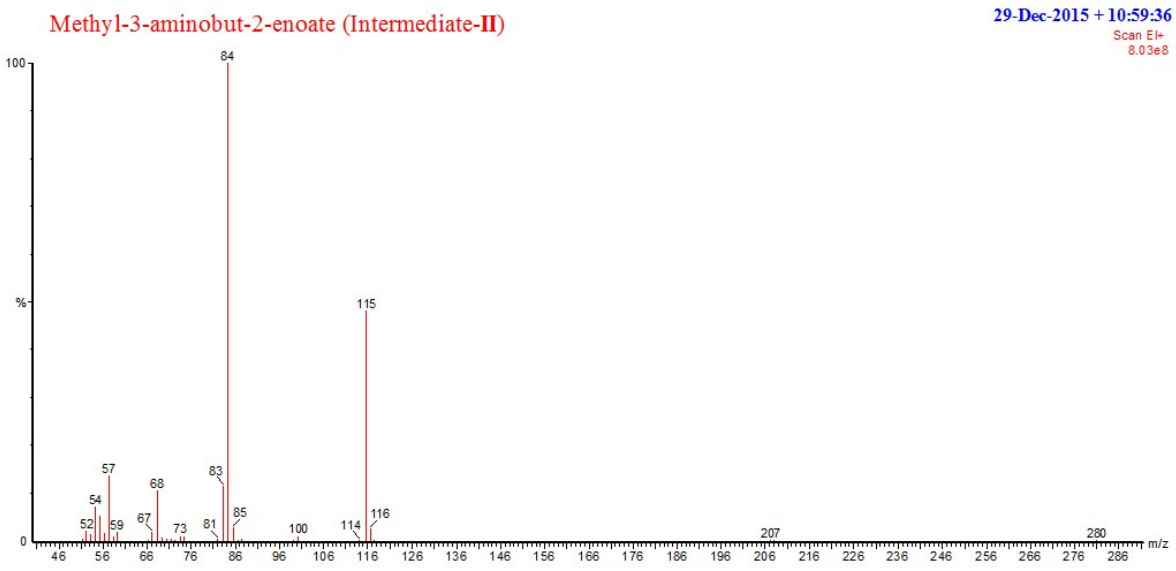

Fig. S11 GC-MS chromatogram of methyl-3-aminobut-2-enoate (Intermediate-**II**)